Annual Heat Gain of the Tropical Atlantic Computed from Subsurface Ocean Data[1]

DAVID W. BEHRINGER

Atlantic Oceanographic and Meteorological Laboratories, NOAA, Miami, FL 33149

HENRY STOMMEL

Woods Hole Oceanographic Institution, Woods Hole, MA 02543

(Manuscript received 9 February 1981, in final form 9 July 1981)

ABSTRACT

Charts are presented which show the seasonal and annual rates of heat gain of the tropical North Atlantic Ocean. These rates have been computed using subsurface oceanographic data and wind-stress data. In these computations the interseasonal rates of heat gain are determined primarily by the rate of local heating, and their magnitude, in general, is several times larger than the annual rate. The annual mean rate implies a net heat loss over much of the tropical ocean. The probable mechanism for this heat loss is an annual excess in cooling due to evaporation over heating due to the net incoming radiation. The present results show similarities to some results of previous authors who have based their calculations on bulk aerodynamical formulas and radiation estimates.

1. Introduction

Recent determinations of the net annual heat gain of the tropical Atlantic Ocean differ substantially. Table 1 contains the estimated net annual rate of heat gain as computed by various authors from surface marine meteorological reports, using bulk aerodynamical formulas and radiation estimates. We offer here the results of an attempt to obtain an independent estimate using subsurface oceanographic data and wind-stress data to compute the heat gain through the ocean surface.

About 30 years ago F. C. Fuglister (personal communication) pointed out the strong veering of the temperature gradient with depth in the upper layers of the tropical North Atlantic Ocean. An inspection of temperature charts in standard atlases (Wust, 1936; Bohnecke, 1936) reveals that at the surface the temperature gradient is toward the southwest while at 200 m the gradient is toward the northwest. The phenomenon is apparent also in the fields of seasonally averaged historical temperature data available from the National Oceanographic Data Center (NODC). Fig. 1 shows the temperature gradient computed from these data at several depths for two locations (15°N, 30°W and 15°N, 40°W) and for two seasons (winter and summer).

The veering of the temperature gradient has some clear implications for a simple heat budget calculation. In deeper layers the geostrophic flow is parallel to the isotherms but in the surface mixed layer the geostrophic flow is across the isotherms in the direction of increasing temperature. This by itself would imply a net heat gain by the upper ocean. However, in parts of the tropical North Atlantic Ocean there is a strong Ekman drift toward the north-northwest in the direction of decreasing temperature and this, by itself, would imply a net heat loss. In our calculations we have balanced these competing effects with the effects of local heating and vertical advection to determine the net rate of heat gain of the tropical North Atlantic Ocean.

In the sections which follow we first describe the model for the calculations and the sources of the data. We then discuss in detail the calculations at a sample point (20°N, 40°W). Finally, we show charts of the net rate of heat gain for the North Atlantic Ocean between 0 and 30°N for four interseasonal periods and for the annual average.

2. The heat budget in the mixed layer

Within the mixed layer the temperature, $\theta(x, y, z, t)$ changes with time and heat is absorbed at a rate $q(x, y, z, t)$ per unit volume. At each depth the conservation equation is

$$\frac{\partial \theta}{\partial t} + u\frac{\partial \theta}{\partial x} + v\frac{\partial \theta}{\partial y} + w\frac{\partial \theta}{\partial z} = \frac{q}{\rho C_p}, \quad (1)$$

where the velocities (u, v, w) are the sum of absolute geostrophic and Ekman velocities. In the absence

[1] WHOI Contribution No. 4471.

0022-3670/81/101393-06$05.50

TABLE 1. Comparison of determinations of heat gain in the tropical North Atlantic. (A discussion of the differences shown in the first four rows can be found in Bunker, 1980).

W m^{-2}	30–20°N	20–10°N
Budyko (1963)	17	29
Bunker and Worthington (1976)	16	26
Hastenrath and Lamb (1978)	−8	2
Bunker (1980)	5	14
This study	−6	−7

of information on the vertical distribution of the velocities within the mixed layer we must integrate Eq. (1) vertically over the thickness h of the mixed layer. To simplify the integration we approximate the vertical velocity by a linear profile which varies from w_h at the bottom of the mixed layer to zero at the surface. Also, we represent the temperature within the mixed layer by the sum of a term, $\bar{\theta}(x, y, t)$ which is independent of z and a term which varies linearly in z by a small constant amount $\Delta\theta$. The integrated conservation equation is

$$h\frac{\partial\bar{\theta}}{\partial t} + \frac{\partial\bar{\theta}}{\partial x}\left(\int_{-h}^{0} U_g dz + \frac{\tau_y}{\rho f}\right) + \frac{\partial\bar{\theta}}{\partial y}\left(\int_{-h}^{0} V_g dz - \frac{\tau_x}{\rho f}\right) + \frac{W_h\Delta\theta}{2} = \frac{Q}{\rho C_p}, \quad (2)$$

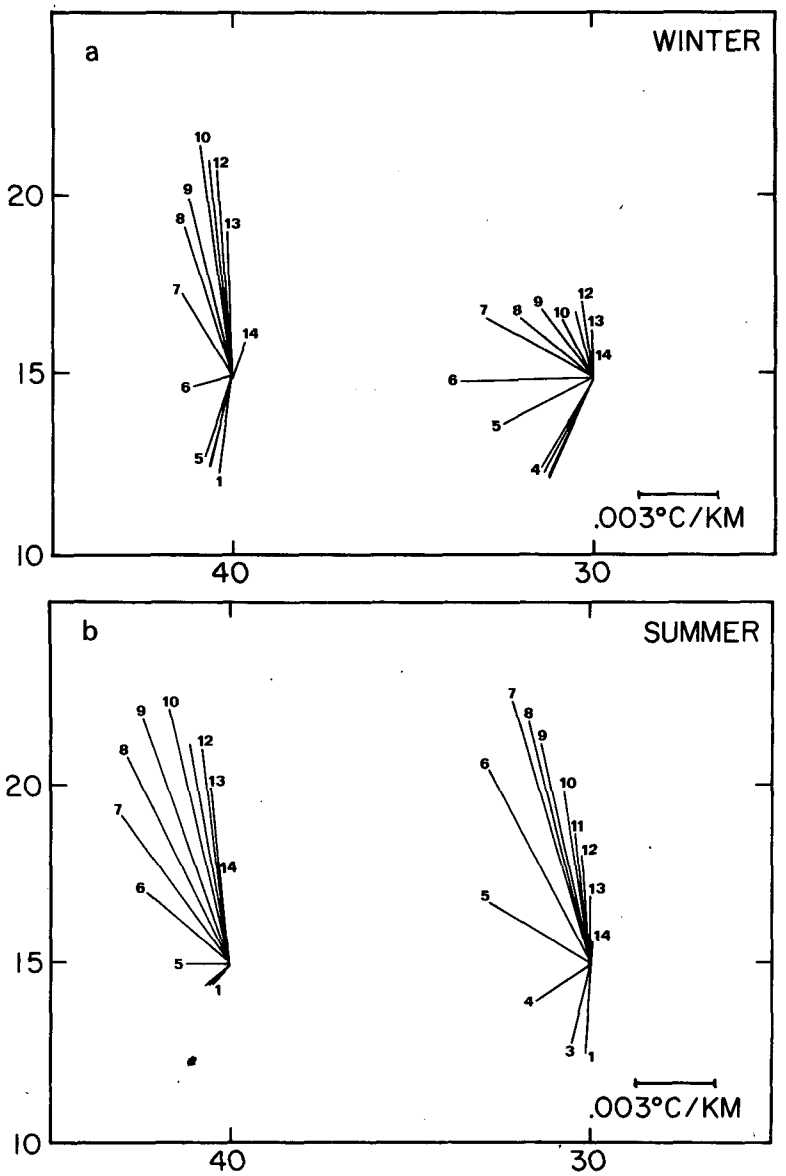

FIG. 1. Direction and magnitude of the horizontal temperature gradient in two regions and two seasons in the tropical North Atlantic. The numerals refer to different depths: 1 = 0 m, 2 = 10 m, 3 = 20 m, 4 = 30 m, 5 = 50 m, 6 = 75 m, 7 = 100 m, 8 = 125 m, 9 = 150 m, 10 = 200 m, 11 = 250 m, 12 = 300 m, 13 = 400 m, 14 = 500 m.

where (U_g, V_g) are the components of the geostrophic velocity vector, (τ_x, τ_y) are the components of the wind-stress vector, f is the Coriolis parameter and Q is the total net rate of heat gain of the mixed layer. The vertical velocity is given by

$$W_h = \frac{\partial}{\partial x}\left(\frac{\tau_y}{\rho f}\right) - \frac{\partial}{\partial y}\left(\frac{\tau_x}{\rho f}\right) - \beta/f \int_{-h}^{0} V_g dz, \quad (3)$$

where β is the gradient of the Coriolis parameter with respect to the y direction.

If we neglect the heat mixed down through the bottom of the mixed layer, then we can interpret Q as the rate of heat gain through a unit area of the sea surface. To compute Q from Eq. (2) we must specify two parameters. One is Z_0, the level of no motion in the geostrophic velocity calculations, and the other is $\Delta\theta$, the vertical variation of temperature in the mixed layer. The parameter $\Delta\theta$ not only appears explicitly in (2) but it is also the criterion by which the mixed layer depth is determined from temperature data. For the calculations described in the following sections we used as standard values, $\Delta\theta = 0.2$°C and $Z_0 = 1000$ m. However, to test the sensitivity of the calculations to these choices we did the computations for all four combinations of the standard choices and the alternate choices, $Z_0 = 700$ m and $\Delta\theta = 0.5$°C. In no case were the results either qualitatively different from or outside of the expected error of the basic calculation.

3. The data and calculations

Before making the calculations we first estimated the temperature, dynamic height and wind-stress for rectangular areas bounded by 2° of latitude and 10° of longitude. For the temperature and dynamic height fields we used monthly averaged station data and XBT data tabulated by the National Oceanographic Data Center. We further averaged the temperature data over 3-month periods and used these and their standard deviations to represent the seasonal fields of temperature and its error. The number of temperature observations per rectangle and season varied greatly, from a few hundreds near the North American coast to a few tens or less in the open ocean, but we encountered only one rectangle for one season in which there were no observations. We computed seasonal dynamic height fields in a similar way but from many fewer observations. Most rectangles contained less than ten dynamic height observations per season and ~12% of them had none at all. The missing data were replaced by linear spatial interpolations. The wind-stress data were obtained from the Woods Hole archives. Leetmaa and Bunker (1978) have discussed these data and they estimated that the error in the wind stress for 2° × 5° rectangles was about ±15–20%; we have assumed an error of ±20% for the same data averaged to our larger rectangles.

These basic fields were used to compute all other fields. We determined the mixed layer depth by setting it equal to the depth at which the temperature had decreased by an amount, $\Delta\theta = 0.2$°C, below the temperature at 10 m. To estimate the error in the mixed-layer depth, we first used the monthly estimates of the mixed-layer depth to compute annual averages and their standard deviations. For most rectangles the standard deviation fell between 20 and 60% of the mean. These standard deviations contain effects of both annual variation and noise which are not readily separable. Therefore, we have simply taken ±40% to be a rough estimate of the error in the mixed layer depth.

We have calculated the various quantities which make up the terms of Eq. (2) at the intersections of the grid defined by the 2° × 10° rectangles of the data fields. Table 2 lists the values of these

TABLE 2. Estimates of quantities for the mixed layer at 20°N, 40°W and for the four seasons. See text for further explanations.

Months	12, 1–2	3–5	6–8	9–11	Units
h	69.0 ± 10.0	54.0 ± 8.0	34.0 ± 6.0	39.0 ± 6.0	10^2 cm
$\bar{\theta}$	23.5 ± 0.4	23.6 ± 0.3	24.9 ± 0.3	26.1 ± 0.3	°C
$\partial\bar{\theta}/\partial x$	−1.09 ± 0.77	−1.08 ± 0.58	−1.27 ± 0.46	−0.75 ± 0.64	10^{-8} °C cm^{-1}
$\partial\bar{\theta}/\partial y$	−2.08 ± 1.47	−2.98 ± 1.14	−2.05 ± 0.89	−1.53 ± 0.97	10^{-8} °C cm^{-1}
$\int_{-h}^{0} U_g dz$	−0.64 ± 0.09	−0.04 ± 0.01	−0.54 ± 0.10	−0.99 ± 0.15	10^4 cm^2 s^{-1}
$\int_{-h}^{0} V_g dz$	−0.77 ± 0.11	−0.62 ± 0.09	−0.73 ± 0.13	−0.60 ± 0.09	10^4 cm^2 s^{-1}
$\tau_y/\rho f$	−0.60 ± 0.04	−0.57 ± 0.05	−0.82 ± 0.06	−0.38 ± 0.03	10^4 cm^2 s^{-1}
$-\tau_x/\rho f$	1.54 ± 0.11	1.64 ± 0.12	1.96 ± 0.14	1.48 ± 0.11	10^4 cm^2 s^{-1}
W_h	−2.47 ± 0.55	−2.14 ± 0.52	−2.41 ± 0.61	−1.91 ± 0.47	10^{-4} cm s^{-1}

TABLE 3. Terms of Eq. (2) at 20°N, 40°W for the four interseasonal periods and the annual period. The units are W m^{-2}.

Term	Winter to spring	Spring to summer	Summer to fall	Fall to winter	Annual
$\rho C_p h \frac{\partial \bar{\theta}}{\partial t}$	2.3 ± 16.5	32.4 ± 9.9	22.6 ± 8.5	−74.8 ± 17.0	−4.4 ± 6.8
$\rho C_p \left[\int_{-h}^{0} U_g dz\right] \frac{\partial \bar{\theta}}{\partial x}$	1.6 ± 0.7	1.4 ± 0.5	3.3 ± 1.3	3.2 ± 1.8	2.4 ± 0.6
$C_p \frac{\tau_y}{f} \frac{\partial \bar{\theta}}{\partial x}$	2.7 ± 1.2	3.5 ± 1.1	2.5 ± 1.0	1.9 ± 1.0	2.7 ± 0.5
$\rho C_p \left[\int_{-h}^{0} V_g dz\right] \frac{\partial \bar{\theta}}{\partial x}$	7.4 ± 2.8	7.2 ± 2.2	5.0 ± 1.9	5.2 ± 2.6	6.2 ± 1.2
$-C_p \frac{\tau_x}{f} \frac{\partial \bar{\theta}}{\partial y}$	−16.8 ± 6.3	−19.0 ± 5.5	−12.9 ± 4.8	−11.4 ± 5.6	−15.0 ± 2.8
$\rho C_p \frac{W_h \Delta\theta}{2}$	−1.0 ± 0.2	−1.0 ± 0.2	−0.9 ± 0.2	−0.9 ± 0.2	−1.0 ± 0.1
Q	−3.9 ± 17.9	24.5 ± 11.6	19.6 ± 10.1	−76.9 ± 18.2	−9.1 ± 7.5

quantities at a sample point, 20°N, 40°W. The mixed layer depth and temperature and the Ekman transports are averages of the data from the eight surrounding rectangles. The averaging produces smoother fields and reduces the error estimates by about a factor of $8^{1/2}$. The horizontal gradients of temperature have been computed from the same eight data points by a simultaneous linear regression of temperature on x and y. The gradients of dynamic height and wind stress involved in computing the geostrophic transports and vertical velocity were computed in a similar way. The error estimates for all these quantities were derived from the error estimates for the original data fields.

4. Results

Table 3 lists the terms of Eq. (2) computed from the numbers in Table 2. The results are shown for the four periods between the seasons and for the annual average. The sum of any column is Q, the net rate of heat gain for that period. Consider first the effect of advection. During every season the southwestward geostrophic transport in the mixed layer is partially opposed by a larger north-northwestward Ekman transport, the net result being a total transport to the northwest in the direction of decreasing mixed-layer temperature. Consequently, the sum of the terms 2–5 in Table 3 is negative and this is reinforced by term 6, representing vertical advection. The negative sum of these terms suggests that advection always supplies heat to this location (20°N, 40°W), at a rate between a minimum of 2 W m^{-2} during the period fall to winter and a maximum of 8 W m^{-2} during the period spring to summer.

Next, consider the changes in the local heat storage due to the local heating of the mixed layer (term 1). During the period from winter to spring, the advection of heat is sufficient to account for the small local rate of heating and also to supply a surplus of heat which presumably is lost to the atmosphere. However, during the remaining interseasonal periods the local rate of heat gain (or loss) by the mixed layer is several times too large to be accounted for by advection; instead it must be explained by local heat exchange with the atmosphere. This last result is consistent with the demonstration by Gill and Niiler (1972) that seasonal heat storage is predominantly local.

The last column of Table 3 shows the annual averages of the terms. As for each of the interseasonal periods the advective terms taken by themselves suggest an annual loss of heat to the atmosphere. This loss is reinforced by the annual average of the local heating term. This term which is one part of the average local rate of heat storage, in general, is not zero. If instead of the advective conservation equation (2) we had used an equation for the heat flux divergence, the annual average of the local heating term would have been balanced by the annual average of changes in the local heat storage due to variations in the mixed layer depth.

Five maps of the net rate of heat gain, Q(W m^{-2}) are shown in Fig. 2: four interseasonal maps and one annual map (average of the first four). South of 10°N our computed values are influenced by the equatorial singularities in the computations of vertical velocity and Ekman and geostrophic transports and we have no confidence in them. North of 10°N the relative magnitudes of the terms in the heat budget equation are similar to those shown in Table 3. However, the sum of the horizontal advective terms does change sign; it is negative to the southwest but becomes positive to the northeast as the Ekman transport weakens.

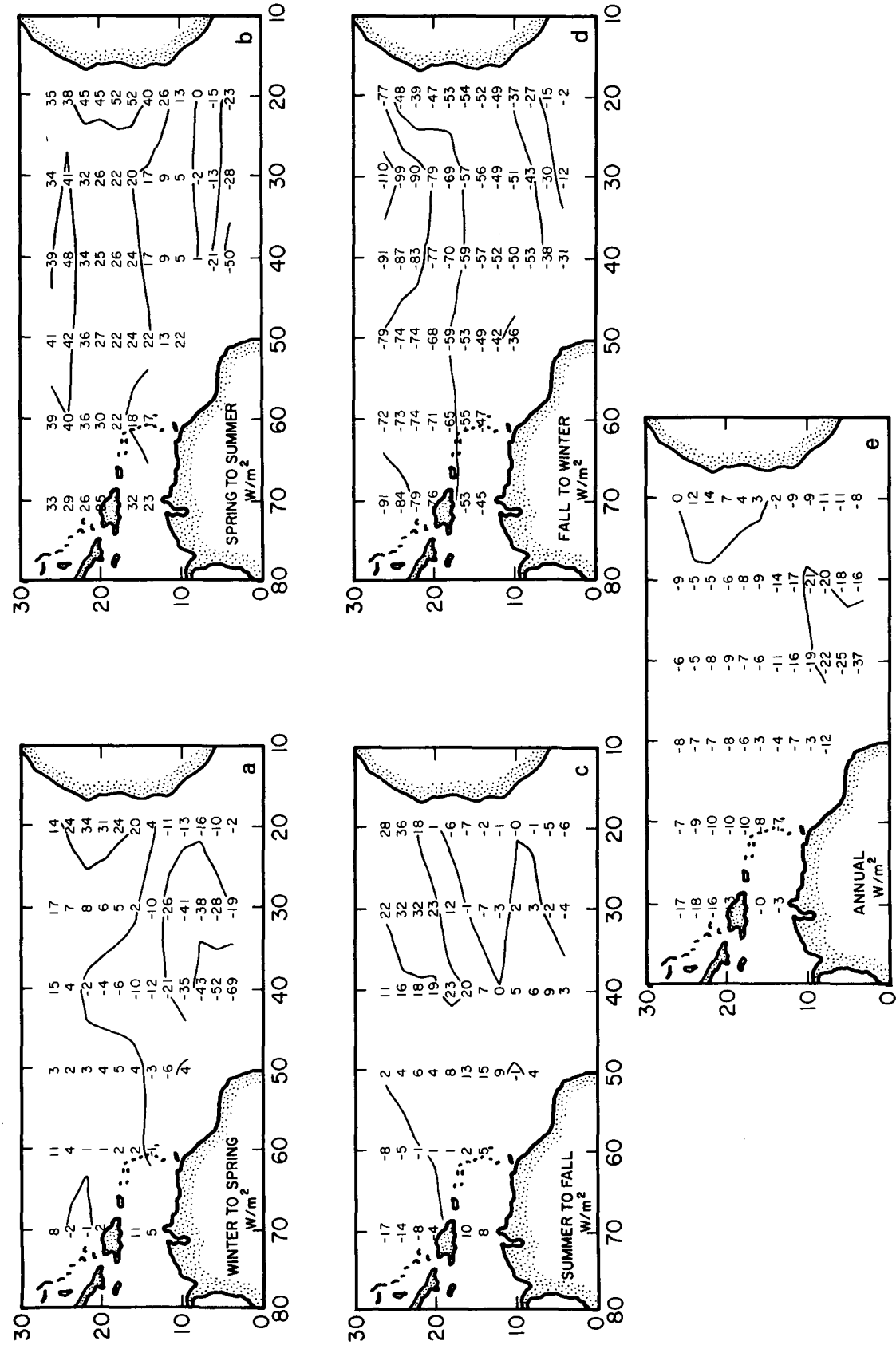

FIG. 2. Maps of the net rate of heat gain interseasonally and averaged for the whole year. The units W m^{-2} and the error estimate is ±7 W m^{-2}; (a) winter–spring; (b) spring–summer; (c) summer–fall; (d) fall–winter; and (e) annual.

The patterns of heat gain shown in the interseasonal maps (excepting the winter to spring period) are dominated by the effects of local heating and cooling. The pattern of heat gain shown in the annual mean map is essentially determined by the mean horizontal heat flux divergence (the contribution from the vertical advection of heat is small north of 10°N). The region of maximum heating (cooling) occurs where the total transport in the mixed layer is strongest in the direction of increasing (decreasing) temperature. The present calculation of the annual pattern of heat gain (north of 10°N) is similar to that depicted by previous authors (Hastenrath and Lamb, 1978; Bunker, 1980) but, as shown by the summary zonal averages in Table 1, our actual values are closer to those of Hastenrath and Lamb (1978) than to those of Bunker (1980) and earlier determinations.

The most striking result of our calculations is the annual loss of heat over much of the tropical ocean. The mechanism for the loss of heat is presumably an annual excess in cooling due to evaporation over heating due to the net incoming radiation at the sea surface. The bulk aerodynamical calculations and radiation estimates of Hastenrath and Lamb (1978) suggest that this mechanism does work over much of the tropical ocean and that, of course, leads to the general agreement between their results and those presented here.

REFERENCES

Bohnecke, G., 1936: Atlas zu: Temperature, salzgehalt und dichte an der oberflache des Atlantischen Ozeans. Band V—Atlas. Wiss. Erg. der Deutschen Atlantischen Exped. "METEOR". Expedition 1925–1927. Verlag Von Walter De Gruyter & Co., 7 pp. + 74 plates.

Bunker, A. F., 1980: Surface energy exchanges of the South Atlantic Ocean. Preprint.

——, and L. V. Worthington, 1976: Energy exchange charts of the North Atlantic Ocean. *Bull. Amer. Meteor. Soc.*, **57**, 670–678.

Budyko, M. I., 1963: *Atlas of the Heat Balance of the Earth*. Kartfabrika Gosgeoltehizdata, Leningrad, 75 pp.

Gill, A. E., and P. P. Niiler, 1972: The theory of the seasonal variability in the ocean. *Deep-Sea Res.*, **20**, 141–177.

Hastenrath, S., and P. J. Lamb, 1978: *Heat budget Atlas of the Tropical Atlantic and Eastern Pacific Oceans*. University of Wisconsin Press, 104 pp.

Leetmaa, A., and A. F. Bunker, 1978: Updated charts of the mean annual wind-stress, convergence in the Ekman layer, and Sverdrup transports in the North Atlantic. *J. Mar. Res.*, **36**, 311–322.

Wust, G., 1936: Atlas zur schichtung und zirkulation des Atlantischen Ozeans. Band VI—Atlas Teil A u. B. Wiss. Erg. der Deutschen Atlantischen Exped. "METEOR". Expedition 1925–1927. Verlag Von Walter De Gruyter & Co., 103 plates.